

Will be published in "Astronomy Letters", 2011, v.37, N7, pp. 483-490

Observations of Lensed Relativistic Jets as a Tool of Constraining Lens Galaxy Parameters

T.I.Larchenkova^{1,*}, N.S.Lyskova² and A.A.Lutovinov^{3,}**

*Astro Space Center, Lebedev Physical Institute, Russian Academy of Sciences,
Profsoyuznaya str., 84/32, Moscow, 117997 Russia¹*

*Moscow Institute of Physics and Technology, Institutskii per. 9, Dolgoprudnyi, Moscow
obl., 141700 Russia²*

*Space Research Institute, Russian Academy of Sciences, Profsoyuznaya str., 84/32,
Moscow, 117997 Russia³*

Received on 25 January 2011

The possibility of using lensed relativistic jets on very small angular scales to construct proper models of spiral lens galaxies and to independently determine the Hubble constant is considered. The system B0218+357 is used as an example to illustrate that there exists a great choice of model parameters adequately reproducing its observed large-scale properties but leading to a significant spread in the Hubble constant. The jet image position angle is suggested as an additional parameter that allows the range of models under consideration to be limited. It is shown that the models for which the jet image position angles differ by at least 40° can be distinguished between themselves during observations on very small angular scales. The possibility of observing the geometric properties of lensed relativistic jets and measuring the superluminal velocities of knot images on time scales of several months with very long baseline space interferometers is discussed.

Key words: relativistic jets, gravitational lensing, B0218+357

* e-mail: tanya@lukash.asc.rssi.ru

** e-mail: aal@iki.rssi.ru

INTRODUCTION

Investigating the physical properties and formation mechanisms of large-scale relativistic jets from active galactic nuclei, radio galaxies, and quasars is one of the most important problems in modern astrophysics. In particular, studying the structure and dynamics of the central regions of extragalactic synchrotron sources, including the study of regions with sizes of the order of several Schwarzschild radii in which relativistic particles observed as extended jets are ejected (Meier 2009), will be a priority direction of research with very long baseline space interferometers (Kardashev 2009) planned to be launched in the immediate future.

The gravitational lensing of galactic nuclei, quasars, and compact regions of radio galaxies with largescale relativistic jets allows these distant astrophysical objects to be observed even now (Nair et al. 1993; Patnaik et al. 1993, 1995). In the immediate future, as the resolution of the instruments used increases, it will allow individual features of their jets, for example, the counterjet unobservable in the absence of lensing, to be also studied. Observing the lensed images of a relativistic jet whose knots move with superluminal velocities due to a small angle between the line of sight and the jet direction gives an unique opportunity to measure the velocity of such bright knots in shorter time intervals than for unlensed jets.

Apart from the questions related to the investigation of physical properties of the jets themselves in gravitationally lensed systems, the questions related to the possibility of constraining the model parameters describing the surface density distribution in the lens and its position relative to the emission source are also interesting. Limiting the number of models, in turn, will allow the most important cosmological parameter, the Hubble constant, to be more properly estimated from observations of the most compact gravitationally lensed systems in which the position of the spiral lens galaxy cannot be determined with present-day instruments. The source B0218+357 ($z = 0.96$; Patnaik et al. 1993, 1995), for which the time delay between the compact core images has been measured with a good accuracy (Biggs et al. 1999; Cohen et al. 2000), but there is an uncertainty in determining the relative positions of the lens and the source (York et al. 2005), is an example of such a gravitationally lensed system.

It should be noted that the lensed jet images retain the geometric shape of the jet on scales of tens of microarcseconds (μas), i.e., the spatial structure in the images on such scales does not change, but, depending on the model of a gravitationally lensed system, the jet image position angles change (see, e.g., Larchenkova et al. 2011), whose values can be used as an additional parameter in modeling. Observations with space interferometers on very small angular scales (tens of μas) will allow this parameter to be measured. This will lead to a limitation of the number of possible models and, as a result, to a more accurate determination of the Hubble constant.

In this paper, which is a logical continuation of our previous paper (Larchenkova et al. 2011), we use the source B0218+357 as an example to consider the problems announced above and the approaches to their solution. The questions related to the choice of models for the mass distribution and position of the lens galaxy that allow the observed large-scale picture of lensing to be adequately reproduced, in particular, the separation between the source's

compact core images, the intensity ratio of these images, and the ringlike structures, are discussed in Section 1. We show that it is necessary to take into account the finite width of the relativistic jet when comparing its modeled images with observational data. The conditions under which the position angles of the jet images on very small angular scales can be measured with an accuracy high enough to constrain the model parameters for the gravitationally lensed system being studied are investigated in Section 2. In Section 3, we present our calculations of the velocity of bright knots in the jet images depending on the model of the lens mass surface density distribution and compare the derived visibility functions. Our results are briefly discussed in the last section.

1. ALLOWANCE FOR THE FINITE JET WIDTH AND COMPARISON WITH VLA OBSERVATIONS

Previously (Larchenkova et al. 2011), we modeled the multiple images of a jet emerging when it is lensed by a spiral galaxy whose surface density was specified by three multicomponent models reflecting the structure of spiral galaxies. We showed that within the framework of the proposed models for the gravitationally lensed system B0218+357 there exists a fairly wide choice of model parameters adequately reproducing its observed properties (the intensity ratio of the compact source’s images A and B $I_A/I_B \simeq (3.1 - 3.7)$, the image separation $\simeq 335$ mas, and the direction of the large-scale jet) but leading to a significant spread in the Hubble constant. In contrast, the semiring structure observed in the radio band and produced by the lensing of the large-scale jet appears only for a limited set of jet parameters and direction. The lens galaxy is represented as a singular disk truncated at a characteristic distance a_d from the center and placed in an isothermal halo with a characteristic size a_h (Keeton and Kochanek 1998). In this case, the contribution from dark matter to the rotation curve at distances $R < a_d$ is taken into account by introducing a coefficient f_d equal to 0.85 (Sackett 1997). The lensing potential, the lens equation, and the expressions for the image magnification and basic parameters (the ellipsoid inclination i , the ellipsoid axis ratio for the disk q_{3d} and halo q_{3h}) used in this model are given in Larchenkova et al. (2011) (Model I).

To illustrate the aforesaid, we chose three sets of model parameters adequately reproducing the observed properties of the source B0218+357, including the presence of a semiring structure:

$$\begin{aligned} i &= 0^\circ, q_{3h} = 0.8, q_{3d} = 0.5, a_d = 1.0, \\ i &= 0^\circ, q_{3h} = 0.6, q_{3d} = 0.45, a_d = 1.0, \\ i &= 10^\circ, q_{3h} = 0.6, q_{3d} = 0.05, a_d = 1.0, \end{aligned}$$

which we will designate below as I, II, and III, respectively. The quantity a_d is expressed in units of the Einstein-Chwolson radius.

Previously (Larchenkova et al. 2011), we used the approximation of an infinitely thin jet when modeling gravitationally lensed relativistic jets, i.e., the relativistic jet was represented

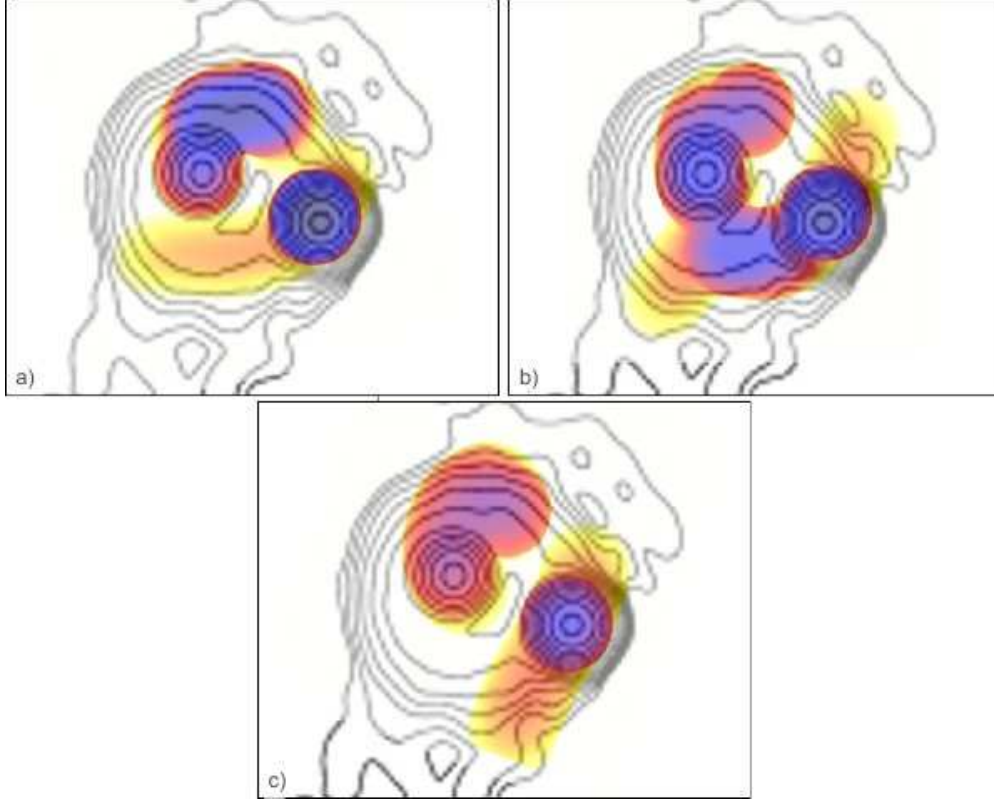


Fig. 1: Comparison of the results of modeling the relativistic jet in B0218+357 (blue corresponds to the maximum intensity, yellow to the minimum) with the results of VLA observations at 15 GHz taken from Biggs et al. (1999) (indicated by contours) for the sets of parameters I (a), II (b), and III (c).

as an infinitely thin segment with a constant intensity at each of its points. However, to properly compare the observational data with the modeling results, it is important to take into account the finite jet width at least for two reasons. First, when an extended source crosses the caustic curve, the magnification of the emerging images is not infinite but depends both on the size of the source itself and the intensity distribution over it and on the properties of the lensing potential (Schneider et al. 1999). Second, the observations are performed with a finite angular resolution, as a result of which any fine details of the images turn out to be blurred.

The parameters of the jet itself, such as the diameter, the position angle, and the intensity distribution along it, the presence and spatial positions of bright knots in the lensing region, are not known for sure for the system under consideration. Therefore, below we use the observed (and rescaled in accordance with the distance) parameters of the nearest and best studied relativistic jet in the source M87 (Sparks et al. 1996; Matveyenko and Seleznev 2011) to compare the modeled and observed large-scale pictures of lensing. In particular, at a distance corresponding to the neighborhood of the caustic crossing by the jet for the three sets of model parameters for the system B0218+357 under consideration, the jet diameter is assumed to be $\simeq 0.02$ Einstein-Chwolson radius ($\simeq 46$ pc or 3.3×10^{-3} arcsec). At the

same time, it should be noted that near the nozzle, i.e., the ejection region of the relativistic plasma flow, the jet width is probably $\simeq 0.05$ pc (see, e.g., Matveyenko et al. 2010). For the source B0218+357, this corresponds to $\simeq 3.6 \times 10^{-6}$ arcsec.

To compare the modeled large-scale picture of gravitational lensing for the source B0218+357 with VLA observations (Biggs et al. 1999), the resolution of this instrument should be taken into account. It is 0.12 arcsec at 15 GHz, which exceeds the jet width in the caustic crossing region by several tens of times. Thus, the bright extended arcs emerging when the jet crosses the caustic curves during observations with the above resolution turn out to be significantly blurred in both intensity and spatial scale.

Figure 1 shows the results of our modeling for the above three sets of parameters performed by taking into account the VLA angular resolution and the maximum magnification near the caustic crossing by an extended (in both length and width) jet with a constant intensity at each of its points (Schneider and Weiss 1986; Keeton et al. 2003) against the background of the VLA map for B0218+357 at 15 GHz (Biggs et al. 1999). Since the distributions of the intensity and bright knots along the jet (which are observed in large-scale relativistic jets and whose flux is lower than the observed core flux only by several times; see, e.g., Sparks et al. (1996) for M87) for the system under consideration are unknown, we performed our modeling by assuming the absence of bright knots whose images will also be blurred and will not change significantly the large-scale jet image.

We see from Fig. 1 that, apart from quantitative relations between the compact core images, extended structures that to a certain extent correspond to the observed ones can be obtained for all sets of parameters under consideration. In this case, different values of the Hubble constant are obtained for different sets: $H_0(I) = 35.8 \text{ km s}^{-1} \text{ Mpc}^{-1}$, $H_0(II) = 46.3 \text{ km s}^{-1} \text{ Mpc}^{-1}$, $H_0(III) = 68.8 \text{ km s}^{-1} \text{ Mpc}^{-1}$. Thus, additional observed parameters should be introduced to properly determine its value. The position angle of the jet image near the nozzle accessible to observation with very long baseline space interferometers can be one of such parameters.

2. POSITION ANGLES OF THE JET IMAGES NEAR THE EJECTOR OF RELATIVISTIC PARTICLES

According to the VLBA survey of extragalactic sources (Kovalev et al. 2005) for B0218+357 on maximum projected baselines of this ground-based interferometer (440×10^6 wavelengths), whose angular resolution is comparable to the VLBI one, the correlated flux density does not decrease to zero but is about 200 mJy. Therefore, observations of this source with very long baseline space interferometers seem interesting from the viewpoint of determining the structure and direction of the relativistic jet at very small angular distances from the nozzle (the ejector of relativistic particles). Let us consider the possibility of using such observations of the jet images to refine the model of a gravitationally lensed system followed by the refinement of the Hubble constant.

As the limiting cases, Figs. 2a and 2b show the intensity distributions along and across one of the jet images (the set of parameters I). The length of the unlensed jet is $30 \mu\text{as}$ from

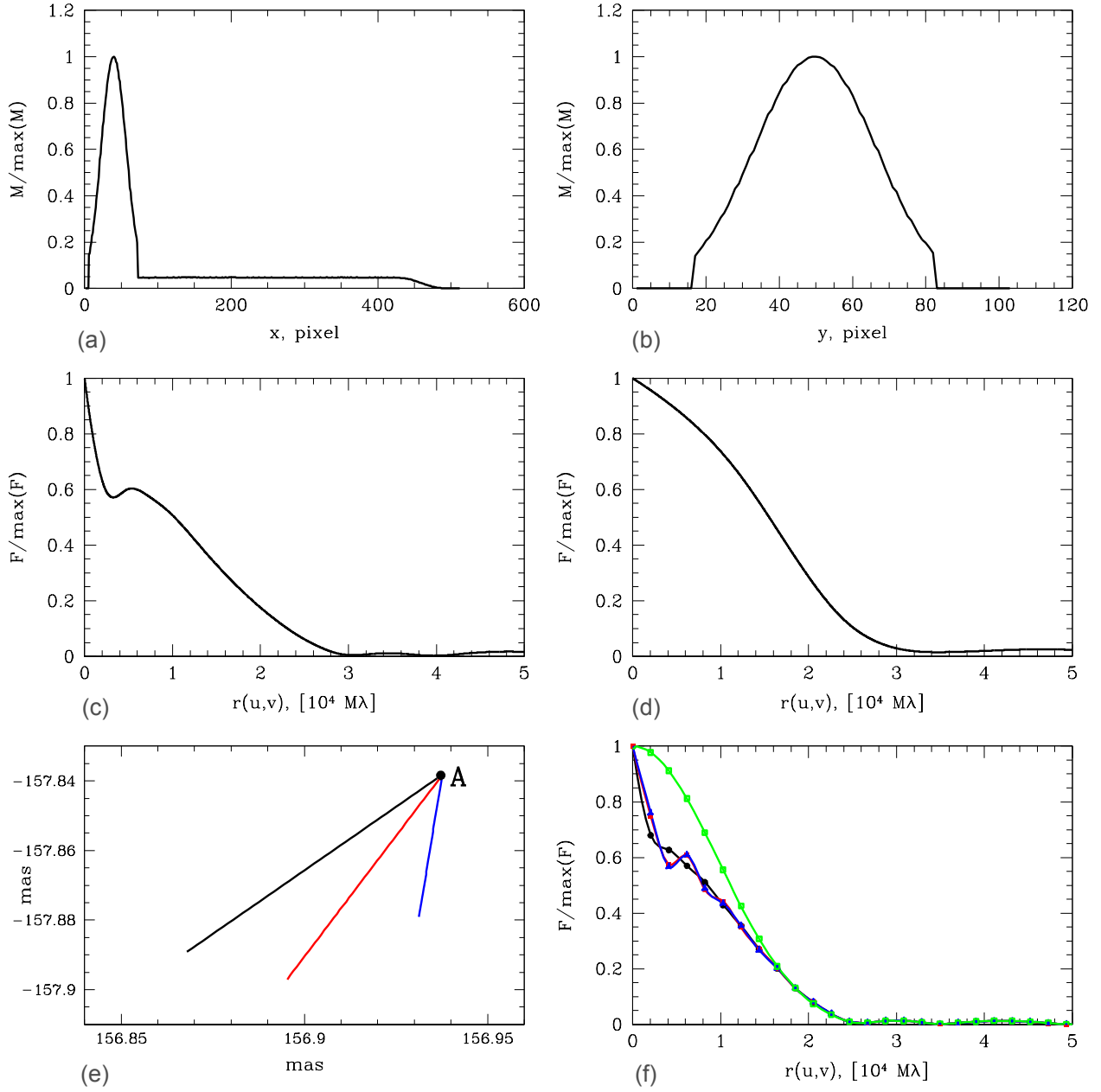


Fig. 2: Intensity distributions along (the X axis) and across (the Y axis) the jet images (a), (b) and the corresponding visibility functions (c), (d). The initial phase ($30 \mu s$) of the relativistic jet emerging from image A (e) and the corresponding visibility functions (f) for the three sets of model parameters: I (black line), II (red line), and III (blue line). The coordinates from the lens position in mas are indicated along the axes. For comparison, the green line indicates the image visibility function for a jet directed at an angle of 90° eastward to model III.

the nozzle (while the length of the image itself turns out to be larger due to the gravitational lensing effect); the intensity distribution across the jet was specified by a Gaussian function with FWHM equal to 0.1 pc ($\simeq 7 \times 10^6$ arcsec); one pixel is equal to one μas . Figures 2c and 2d display the corresponding visibility functions, where the normalized image intensity and the radius vector in the UV-plane in wavelengths are plotted along the vertical and horizontal axes, respectively.

Figure 2e shows the position angle of the jet emerging from the brighter compact core image (image A) for the three sets of model parameters considered. The black, red, and blue lines indicate, respectively, the model with the set of parameters I, for which the jet image position angle is 135° (note that the position angle of the line connecting images A and B is 67° ; Biggs et al. 1999), the model with the set of parameters II and a position angle of 155° , and the model with the set of parameters III and a position angle of 178° . For the convenience of comparison, the initial points of all jets (the position of image A for the compact source) were brought into coincidence at the point corresponding to the position of image A for the set of parameters I. Figure 2f displays the corresponding visibility functions for three jet and nozzle images, which are actually intermediate cases between those presented in Figs. 2c and 2d. We see that for a given angular resolution ($10 \mu\text{as}$) a change in the jet direction by $\simeq 40^\circ$ causes changes in the corresponding visibility functions. The possibility of recording such changes will depend on the signal-to-noise ratio. For comparison, the green line in Fig. 2f indicates the visibility function for a jet with a position angle of -90° . Summarizing the aforesaid, we conclude that the models for which the jet image position angles differ by more than 40° can be distinguished between themselves during observations with very long baseline interferometers.

3. THE VELOCITIES OF KNOTS IN THE JET IMAGES

One more possibility to refine the model parameters for a gravitationally lensed system on very small angular scales is to measure the velocity of the image for a bright jet knot. The superluminal motions of relativistic jets were also measured from the change in the positions of bright knots with time (see, e.g., Jorstad et al. 2001). In the case of gravitational lensing of a jet with a bright knot giving rise to its multiple images, the brighter knot image will move with a velocity higher than both the velocity of the unlensed knot and the velocity of the fainter image. Thus, when such a knot is present in the lensed jet, its displacement can be measured in a shorter time interval than for the unlensed jet.

As the studies showed, the velocity of the knot image depends on the chosen lens model. For example, for a jet segment with a length of $200 \mu\text{as}$ from the nozzle in the case of B0218+357, the sets of parameters I, II, and III give, respectively, velocities along the image of the jet emerging from image A that are a factor of 2.9, 2.4, and 1.4 higher than the velocity v_0 directly along the jet (to be more precise, along the jet projected onto the plane of the sky). Note that the velocities along the fainter image B turn out to be considerably (by several times) lower in all three cases.

Given the velocity with which the knot image moves along the jet and the resolution of

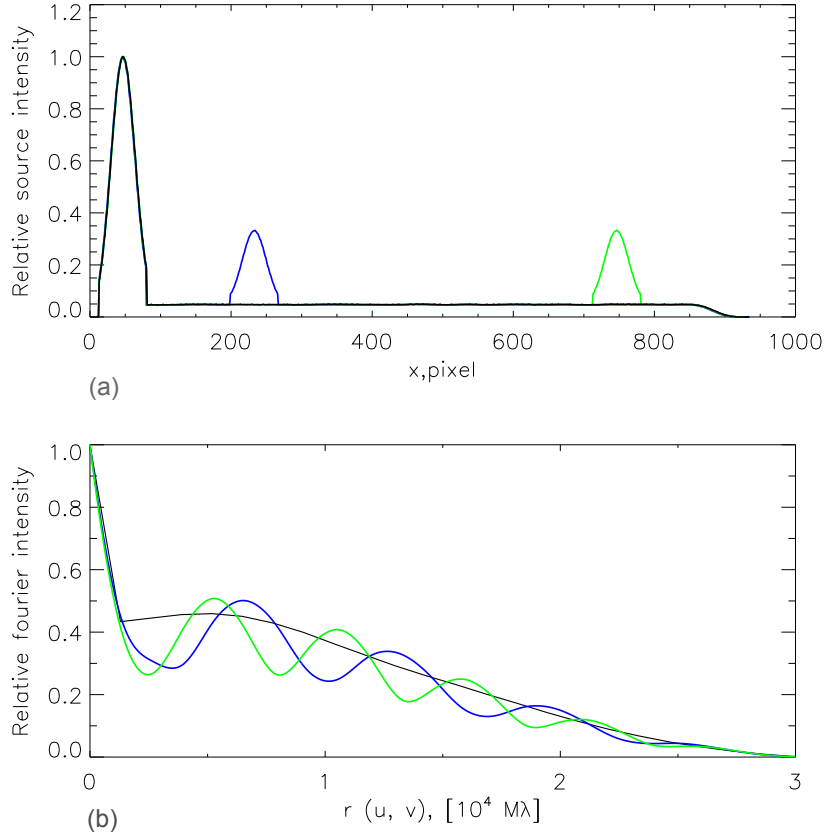


Fig. 3: Intensity distribution (a) and visibility functions (b) for the relativistic jet emerging from image A for the set of parameters I in the following cases: at a uniform intensity (black line), in the presence of a knot with an intensity of $0.3I_A$ at a distance of $\simeq 16 \mu as$ (blue line), and in the presence of a knot with an intensity of $0.3I_A$ at a distance of $\simeq 50 \mu as$ (green line).

the instrument used in the observations, it is easy to determine the time interval after which it is necessary to observe the source to measure this motion. For example, if the velocity along the jet is of the order of the speed of light, then the time interval needed to record the knot displacement at the interferometer’s angular resolution of $\simeq 10 \mu as$ for the model with the set of parameters I is no more than one month.

Since it is not known in advance whether there are bright knots at the angular distance from the nozzle under consideration, the question of whether the visibility functions will be distinguished in the presence of such a bright knot at a certain distance from the nozzle and in its absence becomes interesting. For the set of parameters I and the jet parameters given in the preceding section, we chose three possible realizations for our analysis: (1) a jet with a core and without a bright knot, (2) a jet with a core and a bright knot located at an angular distance of $16 \mu as$ and with an intensity that is a factor of 3 lower than the core one, and (3) a jet with a core and a bright knot located at an angular distance of $50 \mu as$ and with the same intensity as that in case 2. Figure 3 shows the intensity distribution along the jet image and the visibility functions for the three chosen realizations.

We see that the visibility functions for the cases considered in the range of projected space

interferometer baselines from 5×10^9 to 3×10^{10} wavelengths differ significantly from one another and these differences can be recorded at an appropriate signal-to-noise ratio.

4. CONCLUSIONS

Because of small angular separations between the lensed source images, systems where the lens is a spiral galaxy, for example, B0218+357, require modeling to determine the relative positions of the source and the lens, without knowing which, in turn, the Hubble constant cannot be determined. Thus, determining the Hubble constant turns out to be model dependent. This necessitates the introduction of additional model parameters that can be derived from observations on very small angular scales with the goal of limiting the number of possible models. The position angle of the jet images emerging from a region close to the central energy engine and, in the presence of bright knots in this spatial jet region, their velocity in the brightest jet images can be such parameters for gravitationally lensed systems with relativistic jets.

Having modeled the images of the large-scale relativistic jet in the source B0218+357 emerging when it is lensed by a spiral galaxy whose surface density distribution is described by a disk and a softened halo placed in a singular isothermal dark matter halo, we chose several sets of model parameters for the mass distribution and relative positions of the lens and the source that adequately reproduce the observed large-scale picture of lensing. Not only the separation between the source’s compact core images and the intensity ratio of these images but also the extended ringlike structures observed on angular scales of 0.3 arcsec (Biggs et al. 1999) are reproduced for the chosen set of parameters. When compared with the VLA observational data at 15 GHz (Biggs et al. 1999), the modeling results for a fixed relativistic jet diameter with allowance made for the instrument’s angular resolution show good agreement for all of the selected model parameters. Different values of the Hubble constant and different jet image position angles and knot image velocities along the jet correspond to different sets of parameters.

Based on the constructed visibility function for the chosen set of model parameters, we showed using the system B0218+357 as an example that the models for which the jet image position angles differ by at least 40° can be distinguished between themselves during observations on very small angular scales (tens of μas).

Assuming the existence of a bright knot in a region close to the ejector of relativistic particles, we calculated the velocity of the knot image depending both on the velocity of the unlensed knot and on the model of the lens mass surface density distribution, along with the geometry of the gravitationally lensed system, and constructed the visibility functions for a jet without a knot and with a knot located at different distances from the nozzle. The visibility functions for the cases considered were shown to differ from one another in the range of projected space interferometer baselines from 5×10^9 to 3×10^{10} wavelengths.

In addition, for jets with superluminal motions using the sets of parameters considered here, the velocity of the knot image can be measured during observations with an angular

resolution of $\sim 10 \mu\text{as}$ by comparing the observational data obtained with a time interval of one month. Thus, by measuring the displacement of individual bright knots in the images with time, it becomes possible to measure the propagation velocity of the jet within the framework of a specified model for a gravitationally lensed system.

5. ACKNOWLEDGMENTS

We wish to thank L.I. Matveyenko, V.A. Demichev, and N.S. Kardashev for discussions and useful remarks. This work was supported by the “Origin, Structure, and Evolution of Objects in the Universe” Program of the Presidium of the Russian Academy of Sciences, the Program for Support of Leading Scientific Schools (project no. NSh-5069.2010.2), and the State contracts P1336 and 14.740.11.0611.

REFERENCES

1. A. D. Biggs, I. W. A. Browne, P. Helbig, et al., *Mon. Not. R. Astron. Soc.* 304, 349 (1999).
2. A. S. Cohen, J. N. Hewitt, C. B. Moore, and D. B. Haarsma, *Astrophys. J.* 545, 578 (2000).
3. S. G. Jorstad, A. P. Marscher, J. R. Mattox, et al., *Astrophys. J. Suppl. Ser.* 134, 181 (2001).
4. N. S. Kardashev, *Phys. Usp.* 52, 1127 (2009).
5. C. R. Keeton and C. S. Kochanek, *Astrophys. J.* 495, 157 (1998).
6. C. R. Keeton, B. S. Gaudi, and A.O. Petters, *Astrophys. J.* 598, 138 (2003).
7. Y. Y. Kovalev, K. I. Kellermann, and M. L. Lister, *Astron. J.* 130, 2473 (2005).
8. T. I. Larchenkova, A. A. Lutovinov, and N. S. Lyskova, *Astron. Lett.* 37, 233-247 (2011).
9. L. I. Matveyenko, S. S. Sivakon, S. G. Jorstad, and A. P. Marscher, *Astron. Lett.* 36, 151 (2010).
10. L. I. Matveyenko and S. V. Seleznev, *Astron. Lett.* 37, 154 (2011).
11. D. L. Meier, *ASP Conf. Ser.* 402, 342 (2009).
12. S. Nair, D. Narasimha, and A. P. Rao, *Astrophys. J.* 407, 46 (1993).
13. A. R. Patnaik, I. W. A. Browne, and L. J. King, *Mon. Not. R. Astron. Soc.* 261, 435 (1993).
14. A. R. Patnaik, R.W. Porcas, and W. A. Browne, *Mon. Not. R. Astron. Soc.* 274, L5 (1995).
15. P. D. Sackett, *Astrophys. J.* 483, 103 (1997).
16. P. Schneider and A. Weiss, *Astron. Astrophys.* 164, 237 (1986).
17. P. Schneider, J. Ehlers, and E. E. Falco, *Gravitational Lenses* (Springer, Berlin, 1999).
18. W. B. Sparks, J. A. Biretta, and F. Macchetto, *Astrophys. J.* 473, 254 (1996).
19. T. York, N. Jackson, I.W. A. Browne, O.Wucknitz, and J. E. Skelton, *Mon. Not. R. Astron. Soc.* 357, 124 (2005).